

# RECIPROCAL FUNCTIONAL INTERACTIONS BETWEEN THE RESPIRATION/CIRCULATION CENTER, THE UPPER SPINAL CORD, AND THE TRIGEMINAL SYSTEM

Itaru Yazawa\*,  
Seiji Shioda

Department of Anatomy  
Showa University School of Medicine  
1-5-8 Hatanodai  
Shinagawa-ku, Tokyo 142-8555  
Japan

## Abstract

The interplay of neural discharge patterns involved in “respiration”, “circulation”, “opening movements in the mandible”, and “locomotion” was investigated electrophysiologically in a decerebrate and arterially perfused *in situ* rat preparation. Sympathetic tone increased with increases in perfusion flow rate. All nerve discharges became clearly organized into discharge episodes of increasing frequency and duration punctuated by quiescent periods as the perfusion flow rate increased at 26°C. The modulated sympathetic tone at 10x total blood volume/min activated the forelimb pattern generator and spontaneously generated fictive forelimb movement during discharge episodes. The coupling rhythm of respiration and locomotion during motion occurred at frequency ratios ranges of 1:2 and 1:3. Small increases in systemic pressure were always generated after the initiation of motion. Opening movements in the mandible, occurring during the inspiratory phase at all tested flow rates, were generated in both the inspiratory and expiratory phases during motion. Although the central mechanism for the entrainment of respiratory and locomotor rhythms has not been identified, a spinal-feedback mechanism generating fictive locomotion in the upper spinal cord contributed to generating the opening movement in the mandible in the expiratory phase during motion. The existence of this mechanism implies that there is a reciprocal functional interaction between the brainstem and the spinal cord, whereby the intake and output of air by the lungs is efficiently improved during movement by both nasal and mouth breathing. These results suggest that this reciprocal functional interaction plays an important role in increasing oxygenated blood flow during locomotion.

## Keywords

• Discharge episodes • Entrainment • Respiration • Circulation • Locomotion  
• Chemoreceptor discharges • Opening movements of the mandible

Received 22 November 2014  
accepted 19 January 2015

## Abbreviations

ECG - electrocardiogram  
FPG - forelimb pattern generator  
(L-)HGN - (left) hypoglossal nerve  
LPG - locomotor pattern generator  
MA - moving average  
MF - median filtering  
(L-)(R-)MCN - (left) (right) musculocutaneous nerve  
MLR - mesencephalic locomotor region  
PCO<sub>2</sub> - partial pressure of carbon dioxide  
PO<sub>2</sub> - partial pressure of oxygen  
(L-)PHN - (left) phrenic nerve  
SND - sympathetic nerve discharge  
TBV - total blood volume  
(L-)TGN - (left) trigeminal nerve

## Introduction

Entrainment of respiratory and locomotor rhythms during locomotion is a well-documented phenomenon in many species, including rats, cats, rabbits, dogs, and humans [1-5]. Such coupling can be provoked by electrical stimulation of either the mesencephalic locomotor region (MLR) or the subthalamic locomotor region [2, 6] within a range of frequency ratios (e.g., 1:1, 2:1, and 3:2). Although the coordination of respiratory and locomotor rhythms is thought to be generated by either feed-forward [5, 7] or spinal feedback mechanisms [8-12], the central neural mechanisms involved remain poorly understood.

It is clear that the MLR and the respiratory/ cardiovascular networks are located in

overlapping brainstem and midbrain areas [13-15]. Morphological evidence has established connectivity between the brainstem and the spinal cord indicating some functional interactions between the networks in these two areas [16]. The brainstem, especially the reticular formation, has been implicated in the control of motor behaviors, e.g. locomotion [17], respiration [18], and jaw movements [19]. However, although it has been reported that central and peripheral chemoreceptor discharges influence trigeminal, hypoglossal and phrenic motor neurons [20], the coordination of respiratory and trigeminal motor rhythms during locomotion is not well understood.

We previously reported that nerve discharges become clearly organized into discharge episodes of increasing frequency and duration, punctuated by quiescent periods

\* E-mail: yazawa-ns@umin.ac.jp

 © 2015 Itaru Yazawa, Seiji Shioda licensee De Gruyter Open.

This work is licensed under the Creative Commons Attribution-NonCommercial-NoDerivs 3.0 License.

as perfusion flow rate increased at room temperature in decerebrate arterially perfused *in situ* mouse preparations [12]. The hyperoxic/normocapnic state generated by the high flow rates could trigger the locomotor pattern generator and initiate fictive movement during discharge episodes in the hindlimbs and the increase in respiratory rate during locomotion was caused both by impulses from the lower spinal cord (which produces a locomotor-like discharge via ascending pathways) and afferent input received from mechanoreceptors and nociceptors, as discharge episodes originated in the lower spinal cord [12]. The preparation, originally developed by Pickering and Paton [21], is maintained by using artificial cardiopulmonary bypass to deliver oxygen to the body. The oxygen consumption increases with increasing perfusion flow volume in the living body as described in human extracorporeal circulation [22, 23] presumably as metabolism increases when the flow rate increases. However, the increase in metabolism does not always imply neuronal activity and/or sympathetic tone. It is unclear whether the sympathetic tone resulting from the increase in flow rate can generate unknown autonomic functions.

The present study used decerebrate and arterially perfused *in situ* rat preparations and electrophysiological techniques to investigate: (i) whether fictive locomotion in the forelimbs can be autonomously generated by a certain sympathetic tone resulting from an increase in flow rate, (ii) whether rhythm coupling of locomotion and respiration/circulation can be produced during locomotion, (iii) what rhythm coupling of respiration and the opening movements of the mandible can be produced during locomotion, and (iv) the central neural mechanisms of the entrainment of respiratory and locomotor rhythms.

## Experimental procedures

### Animals

Rats were kept in a temperature-controlled room with *ad libitum* access to food and water. The wellbeing of the rats was ensured, and all animal-use procedures were in strict accordance with The National Institutes

of Health (NIH) Guidelines for the Care and Use of Laboratory Animals and were reviewed and approved by the Institutional Animal Care and Use Committee of Showa University.

### Decerebrated and arterially perfused *in situ* rat preparation

Experiments were performed on 60 Wistar rats (Tokyo Experimental Animal Inc., Saitama, Japan) aged 9-24 days and weighting 15.7-61.7 g. Each rat was initially sedated via inhalation of 5.0% isoflurane. During surgery, isoflurane concentration was maintained at 2.0%, and the depth of anesthesia was assessed by respiratory rate and responsiveness to tail pinch. The same surgical procedure as described in our previous study (see [12]) was then used to prepare the decerebrate and arterially perfused *in situ* rat preparation (Fig. 1, yellow dotted-line circle).

After resumption of spontaneous breathing in the *in situ* rat preparation, at  $\leq 5$  min of the initiation of perfusion at 26°C, the muscle relaxant *d*-tubocurarine (2  $\mu$ M) was added to the perfusate to induce immobilization. The left phrenic nerve (L-PHN) was detached from the pulmonary pleura and cut at the distal end. The left and right musculocutaneous nerves (L-MCN and R-MCN), which control the biceps brachii, were carefully detached from the muscles and tissues and then cut at the distal end (Fig. 1B). The trigeminal nerve (TGN), which controls the anterior belly of the digastric muscle, and the hypoglossal nerve (HGN) were carefully detached from blood vessels, muscles and tissues at the mandible and then cut at the distal end (Fig. 1A). The left cervical ganglion was carefully detached from the left subclavian artery at the level of clavicle and then cut at the proximal end (Fig. 1C). Although bradycardia was pronounced at the initiation of perfusion, ventricular fibrillation never developed.

Using a peristaltic pump (model 323U pump, model 318MC pump head; Watson-Marlow, Wilmington, MA, USA), the perfusate was pumped from a reservoir flask into the aortic arch of the preparation through a bubble trap (Yazawa model TK211-054; Unique Medical, Tokyo, Japan) and a nylon net filter (pore size 20  $\mu$ m; Fig. 1), and then recycled from the

recording chamber (Yazawa Model TK211-053; Unique Medical, Tokyo, Japan) back to the reservoir. The flow rate was set to  $\geq 5 \times$  the total blood volume (TBV) per minute at 26°C, with TBV calculated as 1/13 of the body weight in grams [24, 25]. Systemic blood pressure was continuously monitored via the second lumen using a strain-gauge pressure transducer (Pressure Monitor BP-1, World Precision Instruments, Sarasota, FL, USA).

### Extracellular recordings

Suction electrodes constructed of polyethylene tubing (PE 50; Becton, Dickinson and Co., Franklin Lakes, NJ, USA) were used to record neuronal discharge from the L-PHN, left HGN (L-HGN), left TGN (L-TGN), L-MCN and R-MCN, and left middle cervical ganglion. The PHN suction electrode simultaneously recorded the electrocardiogram (ECG). PHN discharge is considered to be output derived from the brainstem respiratory center [26], while changes in heartbeat and systemic pressure are indicators of fluctuations of sympathetic tone in the cardiovascular center of the brainstem [21, 27, 28]. This is because the systemic circuit in this preparation is started at the ascending aorta by the modification of the tip of the catheter and is ended at the incised part of the right atrium. The neuronal discharge from the cervical ganglion is also an indicator of sympathetic tone in the cardiovascular center of the brainstem, which controls the heart and arterioles [27, 28]. The MCN discharge is an indicator of the outputs that are generated in the forelimb pattern generator (FPG), constituting a left/right alternating activity in the spinal network between the fifth cervical and the first thoracic spinal segment [29]. The HGN discharge reveals the inspiratory phase [30] and displays tongue movements [31]. The TGN discharge displays the opening movements in the mandible [32]. The resultant neurograms were amplified 1000 $\times$ , filtered at 1-3000 Hz (DP-304; Warner Instruments LLC, Hamden, CT, USA), and digitized using a PowerLab 4/26 and a Lab chart 7 (AD Instruments Inc., Colorado Springs, CO, USA) at sampling rates of 10,000 Hz. All data were saved on the hard disk of a compatible computer for further analysis.

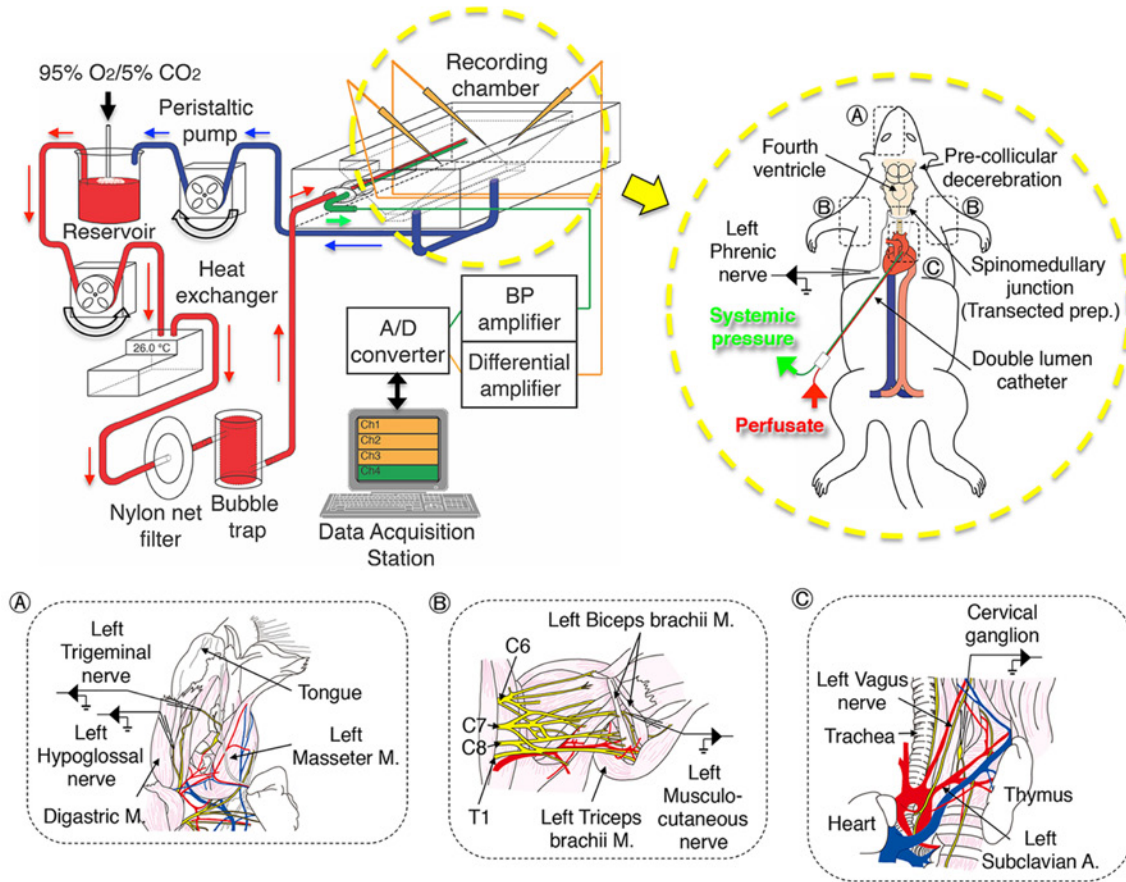


**Figure 1.** The setup of the perfusion circuit used for electrophysiological recordings from the decerebrate and arterially perfused *in situ* rat preparation. The inset in the yellow dotted-line circle is a schematic of a decerebrate and arterially perfused *in situ* rat preparation in which a double-lumen catheter has been inserted into the aortic arch via the left ventricle for perfusion of Ringer's solution. A shows locations of the left trigeminal nerve and left hypoglossal nerve, which were used to record neuronal discharges, and is corresponding to A in the yellow dotted-line circle. B shows locations of the left and right musculo-cutaneous nerves, which were used to record neuronal discharges, and is corresponding to B in the yellow dotted-line circle. C shows locations of the left cervical ganglion, which were used to record sympathetic discharge, and corresponds to C in the yellow dotted-line circle. Note that the liver, the kidney, and the bladder were usually left in place but are not shown here for clarity.

### Data analysis

Neuronal discharges from the PHN, MCN, HGN, TGN, and the cervical ganglion were selected from a recorded sequence. The integrated waveforms were then used to evaluate the phase difference between the ipsilateral and contralateral motor nerves, and to assess the phase-shift between respiratory phases and the opening movements in the mandible. Circular statistics [33] was used to determine the phase difference between the peak amplitudes of the two neuronal discharges during discharge episodes in the L-MCN and R-MCN. In the phase-shift analysis, each cycle period of L-MCN discharge during discharge episodes was measured. Subsequently, the

time lag between L-MCN and R-MCN discharges in the cycle period of the L-MCN discharge was measured. The phase value was calculated by dividing the time lag between the L-MCN and R-MCN discharges in the cycle period of the L-MCN discharge. Each phase value was then multiplied by 360. The values were then plotted on a circle representing the phase difference of possible phases from zero to 360°. The phase values of zero and 360° are equivalent and reflect synchrony, whereas 180° represents alternation. The mean phase and the coupling ratio ( $r$ ) that describes the concentration of phase values around the mean were shown by the direction and the length of the vector originating from the center of the circle. If

the phase relationship of the two discharges were strongly coupled, then phase values would be expected to be highly concentrated around the mean phase. The coupling was considered significant when the Rayleigh test, which determines whether the concentration  $r$  is sufficiently high to state that coupling was present [33], had a  $P$ -value  $< 0.001$ . Circular statistics was also used to investigate the phase shift between the peak amplitude of the two neuronal discharges (i.e. the L-PHN and L-HGN and the L-HGN and L-TGN discharges). The period between the onset of the HGN discharge and the end of the HGN or the PHN discharge was defined as the 'inspiratory phase', while the period between the end of the HGN

or the PHN and the onset of the next HGN discharge was defined as the ‘expiratory phase’. All data compressed to a sample rate of 20 Hz were used.

Raw data were used to assess dependences of neuronal discharges, systemic pressure, and sympathetic tone on the flow rate. Statistical values were expressed as means (SE of the mean). Differences between means were analyzed using a statistical software package (Sigma Stat for Windows; SPSS, Chicago, IL, USA) and assessed by one factor repeated measures anova with a Scheffé *post hoc* analysis. Differences in mean values were taken to be significant at  $P < 0.05$ .

## Results

### 1-1. Dependence of systemic pressure and PHN discharge on perfusion flow rate

Although oxygen consumption increases with increasing perfusion flow volume, as described in human extracorporeal circulation [22, 23], the increase in metabolism does not always indicate an increase in neuronal activity. Thus, the dependence of systemic pressure and PHN discharge on perfusion flow rate was investigated at 26°C.

Figures 2A-(1) and 2A-(2) show typical examples of PHN discharge, the integrated waveform of the PHN (∫PHN) discharge, and systemic pressure, which were generated by various perfusion flow rates. The PHN discharge always showed a ‘eupnoic pattern’ at all the flow rates tested and the ECG was obtained from the PHN recordings. Systemic pressure and the PHN discharge frequency increased with increases in flow rate. Discharge episodes were occasionally observed in the PHN at  $\leq 6 \times$  TBV/min (Fig. 2A-[1]). As the flow rate increased further ( $\geq 8 \times$  TBV/min), the PHN discharges became clearly organized into episodes of increasing frequency and duration, punctuated by quiescent periods (Fig. 2A-[2]). Although the rhythm frequency of PHN discharge increased with the flow rates tested, it increased further when discharge episodes were generated in the PHN. Interestingly, despite the perfusion flow rate being kept constant in the preparation, small increases in systemic pressure were

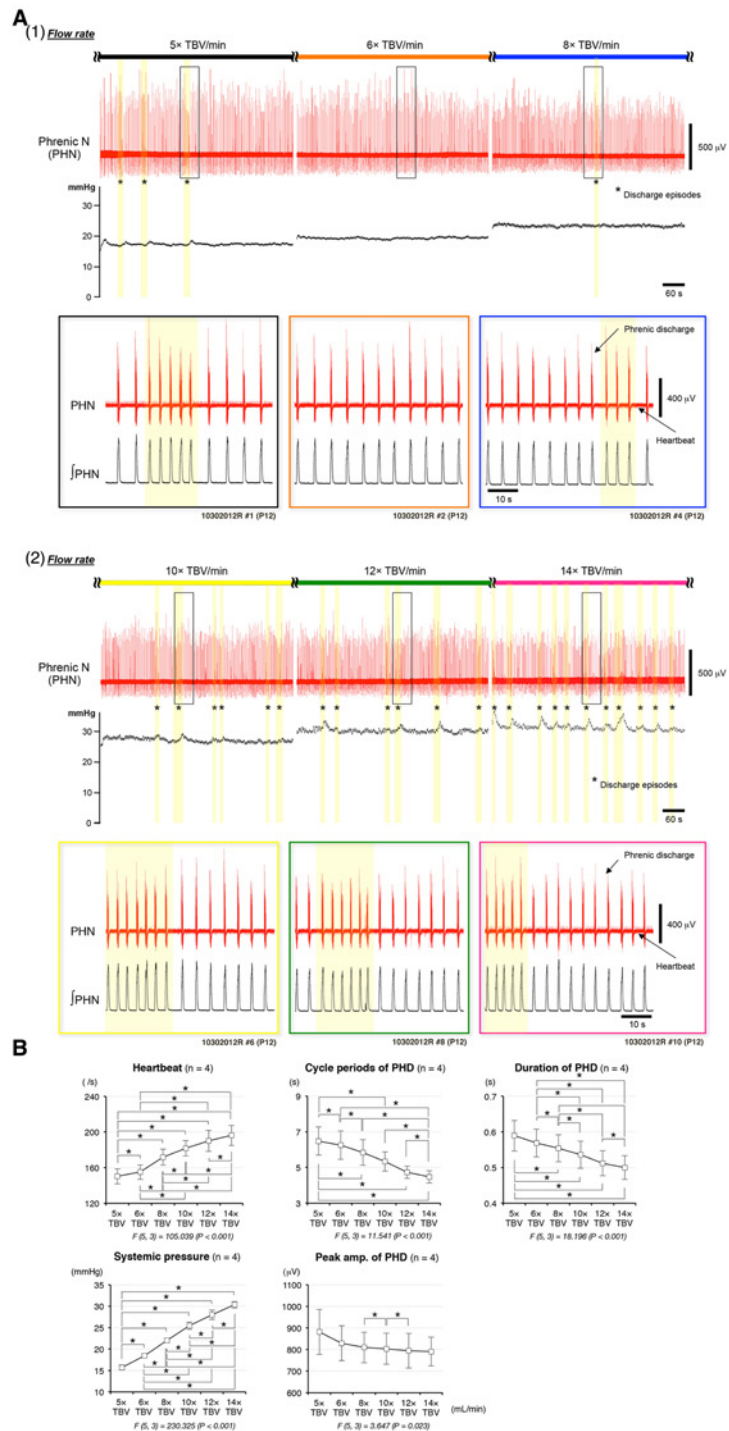


**Figure 2.** A. Typical examples of recordings showing perfusion flow dependence of systemic pressure and PHN discharge. (1) Data collected on perfusion flow dependence at 5x to 8x TBV/min and (2) at 10x to 14x TBV/min. The PHN suction electrode simultaneously recorded the ECG. The systemic pressure was monitored simultaneously (upper panels). The lower panels show an expanded view of the PHN discharge and its integrated waveform of the region surrounding that shown in the upper panels. \* and/or yellow-shaded regions show discharge episodes. All data were obtained from the same preparation made at postnatal day 12. B. Recording periods of 10 min were set for each flow rate and data recorded during the last 5 min were used. All data were obtained from four preparations. The heartbeat increased with the flow rate. The mean (SE) cycle period, duration, and peak amplitude in the PHN discharge decreased with increasing the flow rate. The mean (SE) systemic pressure increased with increased flow rate. \* $P < 0.05$ .

generated when discharge episodes were observed in the PHN (Fig. 2A-[1] and A-[2]). Similar results to those shown in Fig. 2A were reproduced in all cases, regardless of the age of the rat and the experimental conditions ( $n = 50$ ).

We investigated the dependence of systemic pressure, heartbeat, cycle periods of PHN discharge, peak amplitudes of PHN discharge, and durations of PHN discharge, on the perfusion flow rate. Recording periods of 10 min were set for each flow rate and data recorded during the last 5 min were used. All data were obtained from four preparations. In Fig. 2B, the mean heartbeat increased with the flow rate ( $F_{[5,3]} = 105.039$ ,  $P < 0.001$ ) and increased significantly with each increase in flow rate ( $P < 0.05$ ). The mean cycle period, duration, and peak amplitude in the PHN discharge decreased with increasing the flow rate ( $F_{[5,3]} = 3.647$ ,  $P < 0.005$ ;  $F_{[5,3]} = 11.541$ ,  $P < 0.001$ ;  $F_{[5,3]} = 18.196$ ,  $P < 0.001$ , respectively), although the mean cycle period of the PHN discharge did not decrease significantly with incremental increases in flow rate, e.g. from 6x to 10x, from 8x to 10x, and from 10x to 12x TBV/min. The mean duration of PHN discharge decreased significantly ( $P < 0.05$ ) as flow rate increased, but it did not decrease significantly when the flow rate was increased from 5x to 6x TBV/min ( $P > 0.05$ ). When the flow rate was increased from 8x to 10x and from 10x to 12x TBV/min, the mean peak amplitude of PHN discharge decreased significantly ( $P < 0.05$ ). Systemic pressure increased with increased flow rate ( $F_{[5,3]} = 230.325$ ,  $P < 0.001$ ) and increased significantly with each increase in flow rate ( $P < 0.05$ ). Surprisingly, the heartbeat increased significantly with increasing flow rate ( $P < 0.05$ ), although the internal pressure of the heart was always under atmospheric pressure. These results indicate a possibility that the sympathetic tone in the cardiovascular center, which controls heartbeat and vasoconstriction/vasodilation, increases with increasing flow rate.

## 1-2. Dependence of systemic pressure and sympathetic nerve discharge on perfusion flow rate

To confirm that the sympathetic tone in the cardiovascular center increased with increases in flow rate and the increase in systemic pressure

during discharge episodes (as seen in Fig. 2A when it was generated by vasoconstriction of arterioles resulting from increasing amounts of sympathetic discharge [27, 28]), we recorded sympathetic nerve discharges (SNDs) from the left cervical ganglion located at the left clavicle.

Figure 3A shows a typical example of the SND, the integrated waveform of the SND ( $\int$ SND), the moving average (MA) line of the SND ( $\int$ SND MA), and systemic pressure, which were generated by the perfusion flow rates tested. To make the MA line, all data from the integrated waveform of the SND were compressed to a sample rate of 20 Hz and to points (gray dots) using Microsoft Excel software (Microsoft, Redmond, WA, USA). The plot seen in this MA line shows a 60-points

MA for a set of 12,000 data points. The yellow-shading shows the region from the onset of the rise of the  $\int$ SND MA to the peak of the systemic pressure. The  $\int$ SND MA increased with increases in flow rate, indicating that the sympathetic tone in the cardiovascular center increased with flow rate. The increase in sympathetic tone did not always synchronize with the small increases in systemic pressure at 6x TBV/min, presumably indicating that these systemic pressure changes were due to the vibration of the arterioles themselves generated by pulsation of the peristaltic pump. On the other hand, at  $\geq 8x$  TBV/min the increase in the  $\int$ SND MA completely synchronized with the small increase in systemic pressure and

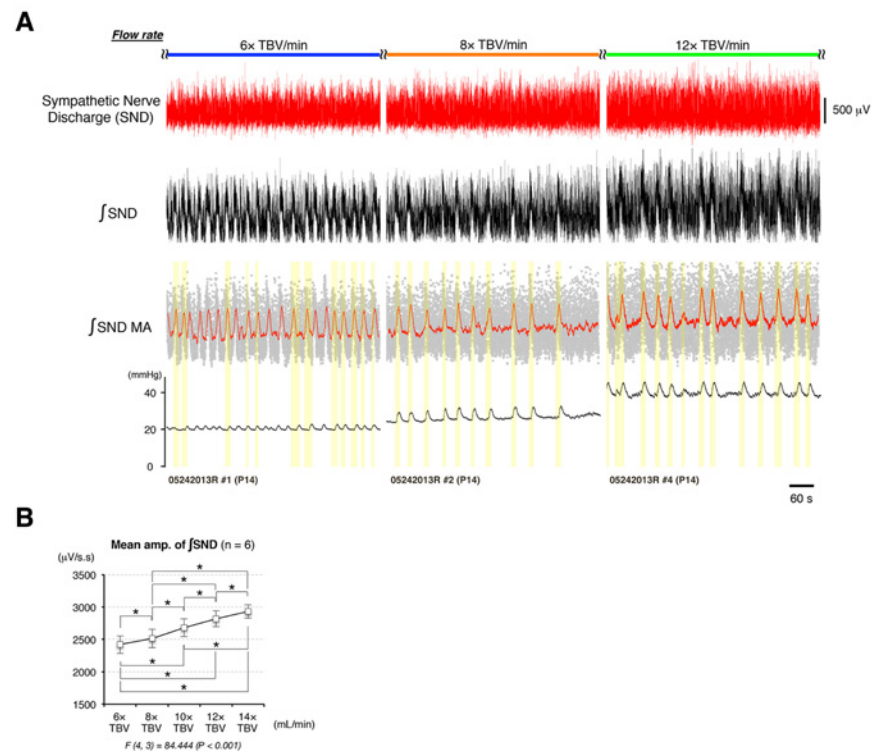


**Figure 3.** Typical examples of recordings showing: (1) the SND increases with increases in the flow rate, and (2) the increase in systemic pressure during discharge episodes is produced by vasoconstriction of arterioles resulting from increasing SND discharge. A. a typical example of the SND (red), the integrated waveform of the SND ( $\int$ SND; black), the moving average (MA) line of the SND ( $\int$ SND MA; red line), and systemic pressure (black), which were generated by various perfusion flow rates tested. The yellow-shaded region shows the region from the onset of the rise of  $\int$ SND MA (red) to the peak of the systemic pressure (black). All data were obtained from the same preparation. Baseline of the  $\int$ SND MA (red) increased with increases in flow rate. All data were obtained from the same preparation made at postnatal day 14. B. Dependence of the peak amplitude of the  $\int$ SND (black). The mean (SE) amplitude of the  $\int$ SND (black) increased with increases in flow rate ( $n = 6$ ).  $*P < 0.05$ . Note that as the flow rate increased, the peak amplitude of the SND increased. Specifically, the amount of the SND increased when small changes in systemic pressure were generated at the flow rate ( $\geq 8x$  TBV/min) tested.

always preceded the small increases in systemic pressure (Fig. 3A). Moreover, we investigated the dependence of the peak amplitude of the  $\int$ SND on the perfusion flow rate (Fig. 3B). Recording periods of 10-15 min were set for each flow rate and data recorded during the last 5 min were used. All data were obtained from six preparations. The mean amplitude of the  $\int$ SND increased with increases in flow rate ( $F_{[4,3]} = 84.444$ ,  $P < 0.001$ ) and it increased significantly with incremental increases in flow rate, i.e. from 6 $\times$  to 8 $\times$ , from 8 $\times$  to 10 $\times$ , and from 12 $\times$  to 14 $\times$  TBV/min ( $P < 0.05$ ). These results indicate that the sympathetic tone in the cardiovascular center of the brainstem increased with increasing flow rate. It is also indicated that the systemic pressure change during discharge episodes at flow rates of  $\geq 8\times$  TBV/min is generated by vasoconstriction or vasodilation of arterioles resulting from increasing or decreasing of the sympathetic tone in the cardiovascular center [27, 28].

## 2. Effect of high flow rates on sympathetic tone

Afferent inputs from peripheral and central chemoreceptors are known to modulate sympathetic/parasympathetic tone in the brainstem [34-37]. In this study, the pH before and after systemic perfusion was maintained within the physiological range, at a mean (SE) of 7.35 (0.05), in all cases ( $n = 60$ ). Thus, the effect of the impulse originating from the pH/PCO<sub>2</sub> sensor, the central chemoreceptor in the respiratory center of the brainstem [35-37] was not examined. Instead, the response of the peripheral chemoreceptor to PO<sub>2</sub> [37] with increases in flow rate was investigated.

Inductions of chemoreflexes were observed in the PHN when a small amount of NaCN (0.1 mL, 1 mM) was administered at 6 $\times$  and 8 $\times$  TBV/min. Conversely, a chemoreflex was not induced when large amounts of NaCN (0.3 mL) were administered at the higher flow rate of 16 $\times$  TBV/min. These results were reproduced in all cases, regardless of the age of the rat and the experimental conditions ( $n = 5$ ). Thus, we concluded that the amount of oxygen delivered to the preparation per unit of time increased with increases in flow rate and a hyperoxic/normocapnic state had been gradually induced

in the preparation by increasing the flow rate and modulating the sympathetic/parasympathetic tone. In addition, we concluded that loss of chemoreponse in the carotid body was due to saturation at 16 $\times$  TBV/min.

## 3. Rhythm couplings of respiration and left/right alternating movements in the forelimbs during discharge episodes

When the sympathetic tone was modulated by a hyperoxic/normocapnic state at high flow rates, discharge episodes of increasing frequency and duration punctuated by quiescent periods were generated in the PHN and bilateral peripheral motor nerves. In discharge episodes, a left/right alternating discharge resulting from activations of the locomotor pattern generator (LPG) was generated in the hindlimb. Simultaneously, the coupling of respiratory and locomotor rhythms occurred at a frequency range ratio of 1:1 in a decerebrate and arterially perfused *in situ* mouse preparation [12].

Therefore, we next investigated whether the modulated sympathetic tone induced by a hyperoxic/normocapnic state could activate the FPG [29] and generate a left/right alternating activity in the forelimbs in a decerebrate and arterially perfused *in situ* rat preparation. Also, we examined changes in the L-PHN and L-MCN and R-MCN discharges, which result from exposing the preparation to transiently hypoxic/normocapnic states by injections of NaCN.

Figures 4A-(1) and 4A-(2) show typical examples of the L-PHN and L-MCN and R-MCN discharges, in response to flow rates of 8 $\times$  and 10 $\times$  TBV/min, respectively. Figure 4A-(3) shows discharges from all three nerves induced by administrations of NaCN at 10 $\times$  TBV/min. In the absence of discharge episodes from any of the nerves, 0.5 mL of 500  $\mu$ M NaCN was administered for 10 s. Figures 4B-(1), 4B-(2), and 4B-(3) provide the expanded views of the integrated waveforms of the L-PHN ( $\int$ L-PHN) and L-MCN discharges ( $\int$ L-MCN) and of the L-MCN ( $\int$ L-MCN) and R-MCN discharges ( $\int$ R-MCN) in the underlined portion (i.e. discharge episodes) in Figs. 4A-(1), 4A-(2), and 4A-(3). Using the time series data of instances of L-PHN and L-MCN discharges during discharge episodes at 8 $\times$

and 10 $\times$  TBV/min and after applying NaCN, circular statistics was used to determine the phase difference from zero to 360 $^\circ$  between the instances of L-PHN and L-MCN discharges and the instances of L-MCN and R-MCN discharges (circular plots in Figs. 4B-[1], 4B-[2], and 4B-[3]). Discharge episodes were observed from all three nerves at 8 $\times$  and 10 $\times$  TBV/min (Figs. 4A-[1] and 4A-[2]). At 8 $\times$  TBV/min, both the L-MCN and R-MCN discharges synchronized to the L-PHN discharge during discharge episodes (integrated waveforms in Fig. 4B-[1]). The phase difference of each peak between instances of L-MCN and R-MCN discharges during discharge episodes was  $\approx 0^\circ$  ( $r = 0.82$ ; circular plots in Fig. 4B-[1]), indicating that these bilateral MCN discharges were respiratory-related. As the flow rate increased (10 $\times$  TBV/min), discharges from all three nerves became more clearly organized into discharge episodes of greater frequency and duration, punctuated by quiescent periods (Fig. 4A-[2]). The rhythm coupling of L-PHN and L-MCN discharges during discharge episodes occurred at frequency ratios ranges of 1:2 and 1:3 (integrated waveforms in Fig. 4B-[2]). The phase difference of each peak between instances of L-MCN and R-MCN discharges during discharge episodes was approximately 180 $^\circ$  ( $r = 0.86$ ; circular plots in Fig. 4B-[2]), indicating that a left/right alternating activity resulting from activation of the FPG was generated in the forelimbs during discharge episodes. Subsequently, NaCN was applied to the preparation at the same flow rate (10 $\times$  TBV/min), to investigate the change of neuronal discharges in the L-MCN and R-MCN in response to transiently increasing amounts of peripheral chemoreceptor discharges. The phase difference between instances of the L-MCN and R-MCN discharges after applying NaCN was 180 $^\circ$  ( $r = 0.79$ ; integrated waveforms and circular plots in Fig. 4B-[3]). Interestingly, the rhythm coupling of respiration and locomotion by a chemoreflex occurred at the frequency ratio range of 1:1 (integrated waveforms in Fig. 4B-[3]). These results indicate that the sympathetic tone resulting from a flow rate of 10 $\times$  TBV/min, which is modulated by a hyperoxic/normocapnic state, can activate the FPG and generate fictive locomotion in the forelimbs during discharge episodes.

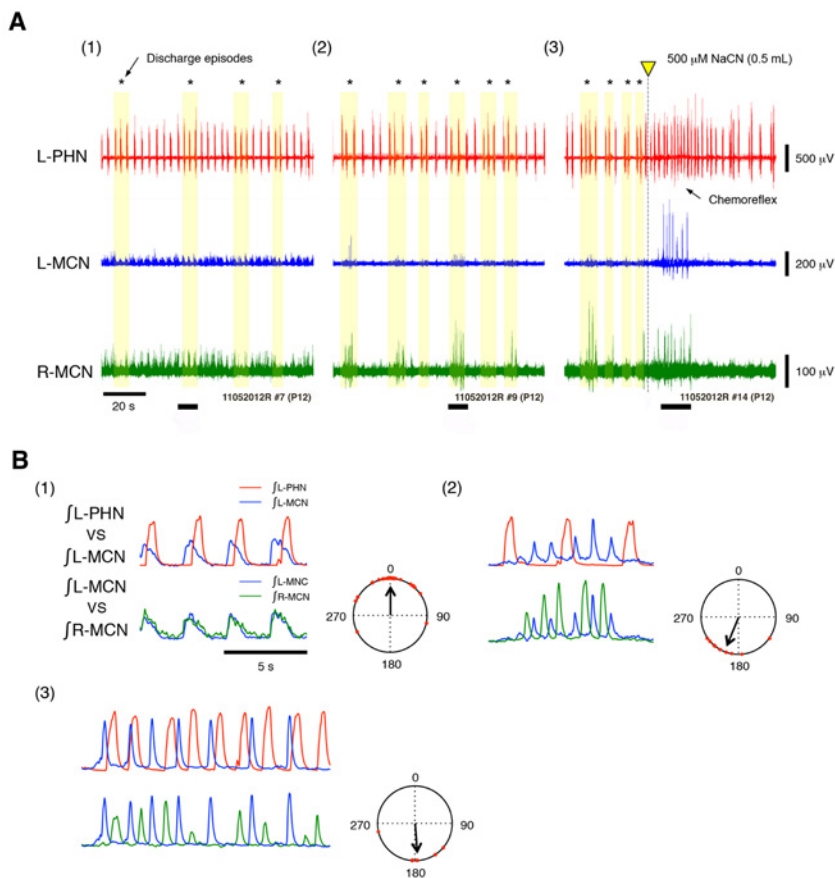


**Figure 4.** A. (1) and (2) typical examples of L-PHN (red) and L-MCN (blue) and R-MCN (green) discharges, in response to flow rates of 8 $\times$  and 10 $\times$  TBV/min, respectively. A (3) shows discharges from all three nerves induced by administrations of NaCN at the same flow rate as set in (2). In the absence of discharge episodes from any of the nerves, 0.5 mL of 500  $\mu$ M NaCN was administered for 10 s (yellow triangle). All data was obtained from the same preparation at postnatal day 12. B. (1), (2), and (3) show the expanded views of the integrated waveforms of the L-PHN ( $\int$ L-PHN; red) and L-MCN ( $\int$ L-MCN; blue) discharges and of the L-MCN ( $\int$ L-MCN; blue) and R-LCN ( $\int$ R-MCN; green) discharges in the underlined portion (i.e. discharge episodes) in A-(1), A-(2), A-(3). Circular statistics was used to determine the phase difference from 0 to 360° between the instances of L-PHN and L-MCN discharges and the instances of L-MCN and R-MCN discharges ( $n = 5$ ).

The results also indicated that the frequency ratio of entrainments of respiration and locomotion changes by the sympathetic tone generated by changing amounts of peripheral chemoreceptor discharges. Similar results to those shown in Figure 4 were reproduced in all cases, regardless of the age of the rat and the experimental conditions ( $n = 5$ ).

#### 4. A left/right alternating activity in the forelimbs generated by the modulated sympathetic tone via descending pathways

To examine whether the left/right alternating activity in the forelimbs seen in Fig. 4 was

generated by impulses originating in the brainstem (i.e. the modulated sympathetic tone) through descending pathways and whether the discharge episodes were generated in the spinal cord, the PHN and L-MCN and R-MCN discharges were recorded at flow rates of 8 $\times$  and  $\geq 10\times$  TBV/min in preparations transected at the spinomedullary junction to sever signal transmission from the brainstem to the cervical spinal cord.

Figures 5A-(1) and 5B-(1) show typical examples of instances of L-PHN and L-MCN and R-MCN discharges, in response to flow rates of 8 $\times$  and  $\geq 10\times$  TBV/min, respectively. Simultaneously, systemic pressure was

monitored. Figures 5A-(2) and 5B-(2) show the  $\int$ L-PHN,  $\int$ L-MCN, and  $\int$ R-MCN discharges, which correspond to the neuronal discharges shown in Figure 5A-(1) and 5B-(1). Figure 5B-(3) shows a typical example of the median filtering (MF) line of the  $\int$ L-PHN,  $\int$ L-MCN, and  $\int$ R-MCN discharges, which correspond to the neuronal discharges shown in Fig. 5B-(2). Median filtering was used to emphasize the neuronal discharges with small amplitudes shown in Fig. 5B-(2) and to remove the neuronal discharges with large amplitudes shown in Fig. 5B-(2). The window width of the smoothing window of PHN and MCN was set at 4001 and 6001 sampling points, respectively. At 8 $\times$  TBV/min, spontaneous neuronal discharge was rarely obtained from the L-PHN. Although it was randomly and simultaneously recorded from both the L-MCN and R-MCN discharges, the rhythm frequency of each spontaneous neuronal discharge was very slow. Systemic pressure resulted in persistent resting hypotension compared with systemic pressure seen in Figs. 2A and 3 (Fig. 5A-[1]). As the flow rate increased further ( $\geq 10\times$  TBV/min), neuronal discharge in the L-PHN became evident, the amplitude increased, and the amounts of L-PHN discharge increased periodically (Fig. 5B-[2]). Although systemic pressure increased with the flow rate, it still resulted in persistent resting hypotension compared with systemic pressure seen in Figs. 2A and 3. On the other hand, neuronal discharges consisting of large and small amplitudes were obtained from the L-MCN and R-MCN. The L-MCN and R-MCN discharges with large amplitudes were simultaneously generated and became clearly organized into discharge episodes of increasing frequency and duration, punctuated by quiescent periods (Fig. 5B-[2]). Interestingly, the neuronal discharge with small amplitudes shown in the L-MCN and R-MCN was produced alternatively and the rhythm frequency of left/right alternating discharge was approximately 1/15 Hz as shown in Fig. 5B-(3) (see Discussion section). Similar results to those shown in Fig. 5 were obtained in all cases, regardless of the age of the rat ( $n = 5$ ).

## 5. Dependence of PHN, HGN, and TGN discharges on perfusion flow rate

We investigated the dependence of PHN, HGN, and TGN discharges on perfusion flow rate to examine whether tongue movements and the mandible opening movements during the inspiratory phase are introduced given a certain sympathetic tone and the airway is maintained in the inspiratory phase [31].

Figures 6A-(1) and 6A-(2) show typical examples of PHN, HGN, and TGN discharges and the integrated waveform of PHN ( $\int$ PHN), HGN ( $\int$ HGN), and TGN ( $\int$ TGN) discharges, which were generated by various perfusion flow rates. The period between the onset of the HGN discharge and the end of the HGN or the PHN discharge was defined as the 'inspiratory phase'. The period between the end of the HGN or the PHN discharge and the onset of the next HGN discharge was defined as the 'expiratory phase'. At  $\leq 7\times$  TBV/min, discharge episodes were rarely generated in the PHN, HGN, and TGN (Fig. 6A-[1]). As the flow rate increased to  $\geq 9\times$  TBV/min, the instances of discharges from all three nerves became clearly organized into discharge episodes of increasing frequency and duration punctuated by quiescent periods, while the rhythm of discharges from all three nerves became more rapid with increasing flow rate (Fig. 6A-[2]). The neuronal discharges from all three nerves were normally generated in the order of the HGN, PHN, and TGN discharges within the inspiratory phase at all flow rates tested (Figs. 6A-[1] and 6A-[2]). Interestingly, when discharge episodes were generated from all three nerves, the TGN discharge was produced in both the inspiratory and expiratory phases (Figs. 6A-[1] and 6A-[2]).

We also examined the dependence of the peak amplitude of the PHN, HGN, and TGN discharges on the perfusion flow rate using the same analysis procedure as used in Fig. 2B. All data were obtained from four preparations. In Fig. 6B, the mean peak amplitude of the PHN discharge decreased as flow rate increased ( $F_{[4, 3]} = 5.804$ ,  $P = 0.008$ ) and decreased significantly as flow rate was increased from  $5\times$  to  $9\times$  TBV/min ( $P < 0.05$ ). The peak amplitude of the HGN discharge showed an increasing trend with increasing flow rate ( $F_{[4, 3]} = 1.221$ ,

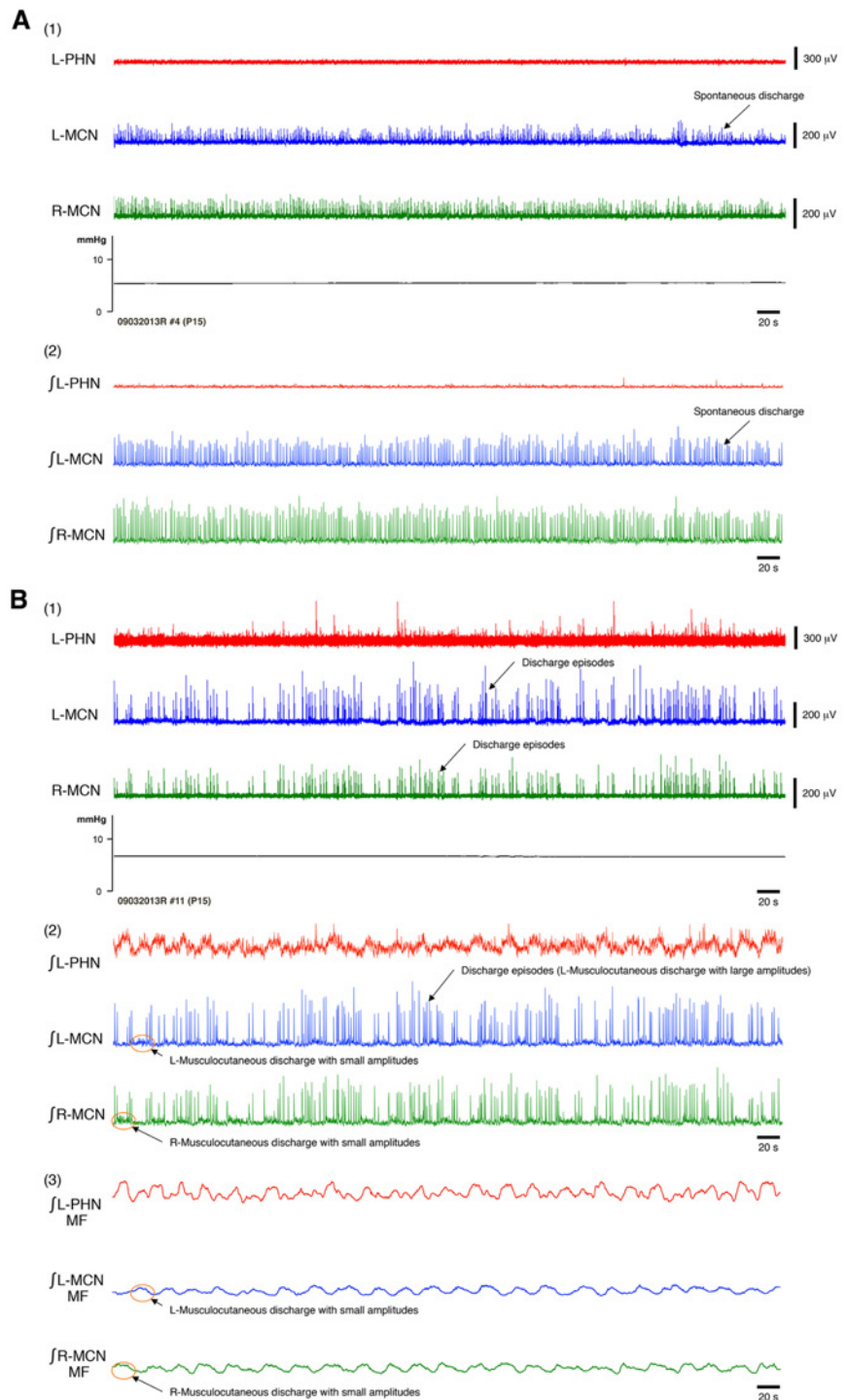


**Figure 5.** A-(1) and B-(1) show typical examples of L-PHN (red), L-MCN (blue), R-MCN (green) discharges, and systemic pressure, in response to flow rates of  $8\times$  and  $\geq 10\times$  TBV/min, respectively, in the preparation transected at the spinomedullary junction. A-(2) and B-(2) show the  $\int$ L-PHN (red), the  $\int$ L-MCN (blue), and the  $\int$ R-MCN (green) discharges, which correspond to the neuronal discharges seen in A-(1) and B-(1), respectively. B-(3) shows the median filtering (MF) line of the  $\int$ L-PHN, the  $\int$ L-MCN, and the  $\int$ R-MCN discharges, which correspond to the neuronal discharges shown in B-(2). All data were obtained from the same preparation made at postnatal day 15.

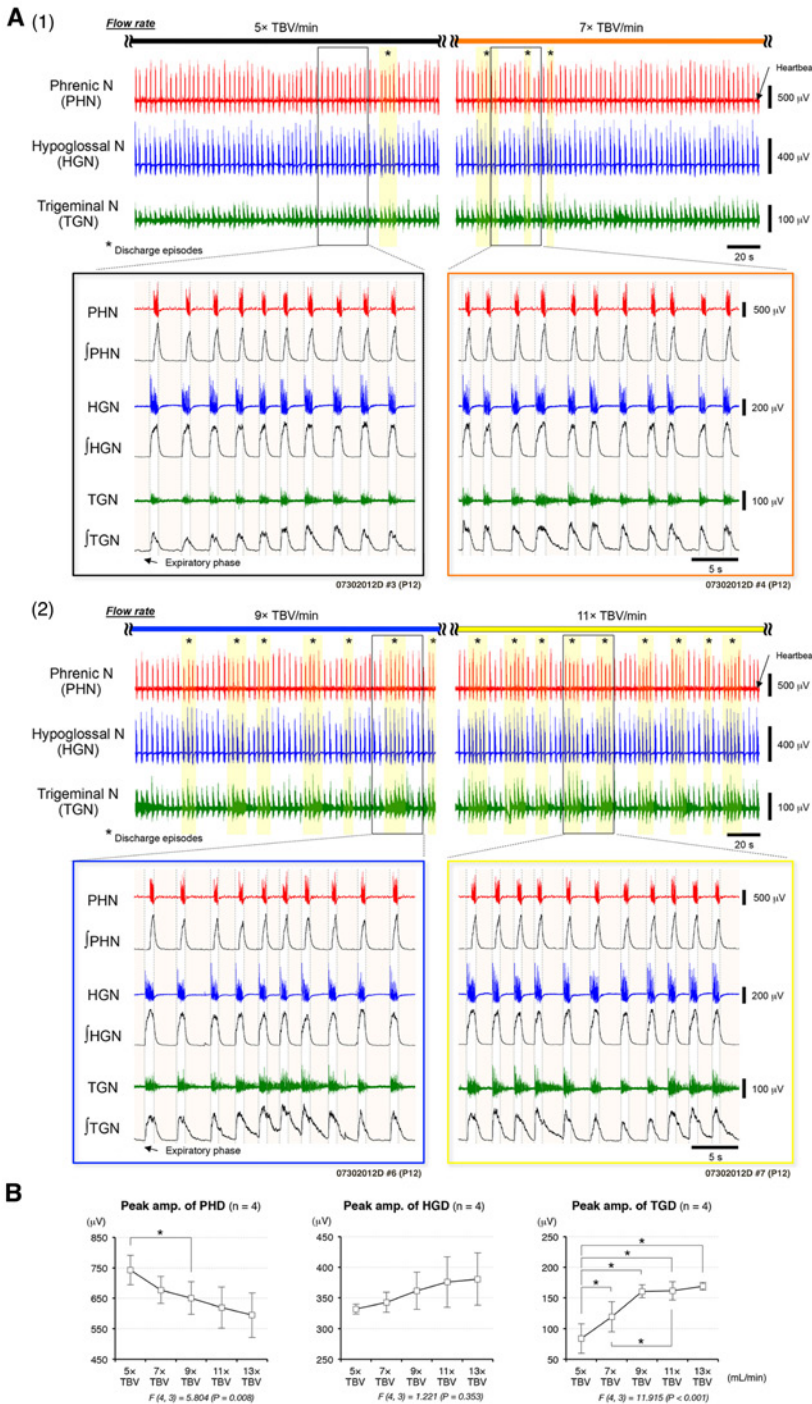


**Figure 6.** A. Typical examples of recordings showing perfusion flow dependence of the PHN (red), HGN (blue), and TGN (green) discharges. All data were recorded from the same preparation. (1) Data collected on perfusion flow dependence at 5x to 7x TBV/min and (2) at 9x to 13x TBV/min. The lower panels present an expanded view of the discharge and its integrated waveform of the region surrounding that shown in the upper panels. \* and/or yellow-shaded regions discharge episodes. The neuronal discharge was always generated in the order of the HGN, PHN, and TGN discharges in the inspiratory phase (white regions in integrated waveforms) at all flow rates tested. All data were obtained from the same preparation made at postnatal day 12. B. The dependence of the mean (SE) peak amplitude of the PHN discharge (PHD), HGN discharge (HGD), and TGN discharge (TGD) on the perfusion flow rate. The same analysis procedure was used as in Fig. 2B. All data were obtained from four preparations. \* $P < 0.05$ .

$P = 0.352$ ). The peak amplitude of the TGN discharge increased with increasing flow rate ( $F_{[4, 3]} = 11.915, P < 0.001$ ) and increased significantly as the flow rate was increased from 5x to 7x, from 5x to 9x, from 5x to 11x, and from 7x to 11x TBV/min ( $P < 0.05$ ). Similar results to those shown in Figures 6A and 6B were reproduced in all cases, regardless of the age of the rat and the experimental conditions ( $n = 25$ ).

### 6. The opening movement in the mandible generated in both the inspiratory and expiratory phases during fictive locomotion

Using the same flow rate as set in the Figs. 4A-(2) and 4A-(3) (10x TBV/min), we investigated the phase relationships between respiration and mandible opening movements during fictive locomotion and the change of neuronal discharges from all of the nerves in response to rapid chemoreflex.

Figure 7A-(1) shows typical examples of the PHN, HGN, and TGN discharges, in response to a flow rate of 10x TBV/min. Figure 7A-(2) shows discharges from all three nerves induced by administrations of 1 mM NaCN (0.5 mL) at the same flow rate. In the absence of discharge episodes from any of the nerves, NaCN was injected for 10 s. Figures 7B-(1) and 7B-(2) show the integrated waveforms of the PHN and HGN, and the HGN and TGN discharges, which correspond to Figs. 7A-(1) and 7A-(2). Using the time series data of instances of PHN, HGN and TGN discharge during discharge episodes and after applying NaCN, circular plot analysis was used to determine the phase shift within the respiratory phase between the instances of PHN and HGN discharge and the instances of HGN and TGN discharge (circular plots in Figs. 7B-[1] and 7B-[2]). All data were obtained from the same preparation made at postnatal day 12.

The discharge episodes were observed from all three nerves at 10x TBV/min (Fig. 7A-[1]). Although the HGN, PHN, and TGN discharges always persisted in the inspiratory phase and were generated in the inspiratory phase outside of discharge episodes (white regions of integrated waveforms in Fig. 7-[1]), the TGN discharge was generated in both the inspiratory ( $r = 0.93$ ; circular plots in Fig. 7B-

[1]) and expiratory phases ( $r = 0.82$ ; circular plots in Fig. 7B-[1]) during discharge episodes. In Fig. 7A-(2), a chemoreflex was generated in the PHN by applying NaCN. At the same time, a rapid neuronal discharge with episodes of greater frequency and duration was produced in the HGN and TGN. The TGN discharge was generated in both the inspiratory ( $r = 0.75$ ; circular plots in Fig. 7B-[2]) and expiratory phases ( $r = 0.95$ ; circular plots in Fig. 7B-[2]) during and after a chemoreflex (circular plots and integrated waveforms in Fig. 7B-[2]). These results indicate that the opening movements in the mandible during fictive locomotion and discharge episodes in the upper limbs were occurring in both the inspiratory and expiratory phases. The same result was obtained in all cases ( $n = 5$ ).

### 7. Phase shifting of opening movements in the mandible to the expiratory phase from the inspiratory phase generated by increasing peripheral and central chemoreceptor discharges

The amplitude of HGN and TGN discharges increases in a hypoxic or a hypercapnic state [20]. However, the phase shifting of opening movements in the mandible to the expiratory phase from the inspiratory phase never occurred. In addition, although the respiratory frequency is stimulated by global central nervous system hypoxia [38], little is known of the relationship between the TGN and HGN and/or PHN discharge in this physiological state. We examined the change in interplay of the PHN, HGN, and TGN discharges in response to increasing peripheral and central chemoreceptor discharges in order to explore the mechanism(s) of the phase shift of opening movements in the mandible to the expiratory phase from the inspiratory phase.

Figure 8A-(1) shows typical examples of PHN, HGN, and TGN discharges in response to a flow rate of  $8 \times \text{TBV}/\text{min}$ . Figure 8A-(2) shows discharges from all three nerves induced by continuous administrations of  $10 \mu\text{M}$  NaCN at the same flow rate ( $8 \times \text{TBV}/\text{min}$ ). The preparation was continuously perfused to increase both the peripheral and central chemoreceptor discharges [38, 39]. Figures 8B-(1) and 8B-(2)

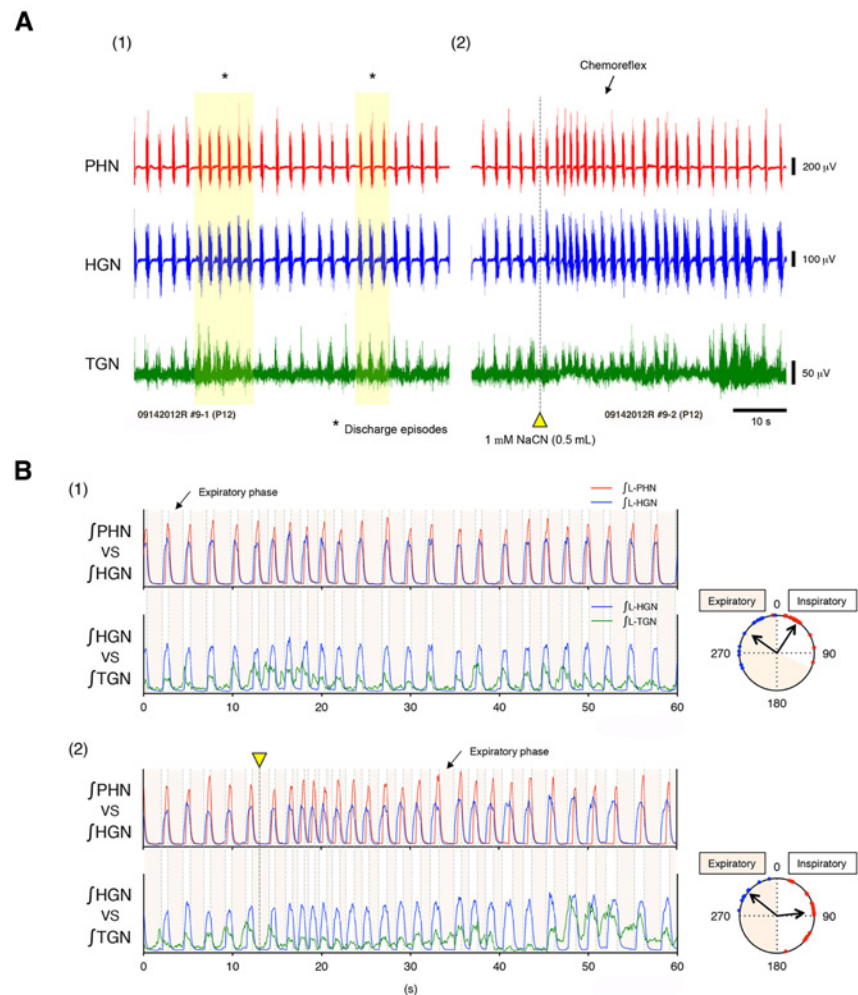


**Figure 7.** A. (1) and (2) show typical examples of PHN (red), HGN (blue), and TGN (green) discharges at the same flow rate as set in Fig. 4A ( $10 \times \text{TBV}/\text{min}$ ), with and without the administration of NaCN. In the absence of discharge episodes from any of the nerves, 0.5 mL of 1 mM NaCN was administered for 10 s (yellow triangle). B. (1) and (2) show the integrated waveforms of the PHN (red) and HGN (blue), and the HGN (blue) and TGN (green) discharges, which correspond to A-(1) and A-(2). All data were obtained from the same preparation at postnatal day 12. The discharge episodes (\* and/or yellow-shaded regions) were observed from all three nerves at  $10 \times \text{TBV}/\text{min}$  (A-[1]).

show the integrated waveforms of discharges from all three nerves, which correspond to Figs. 8A-(1) and 8A-(2), respectively. Circular plot analysis was used to determine the phase shift within the respiratory phase between the instances of PHN and HGN discharge and the instances of HGN and TGN discharge (circular plots in Figs. 8B-[1] and 8B-[2]). All data were obtained from the same preparation made at postnatal day 17. The order of the HGN, PHN, and TGN discharges within the inspiratory phase was kept, and discharges from these three nerves were generated in the inspiratory phase (white regions of integrated waveforms

in Fig. 8B-[1]). The TGN discharge was generated in the inspiratory phase ( $r = 0.98$ ; circular plots in Fig. 8B-[1]). The frequency of discharges from all three nerves was increased by continuous administration of  $10 \mu\text{M}$  NaCN at the same flow rate ( $8 \times \text{TBV}/\text{min}$ ). Although the PHN and HGN discharges were generated in the inspiratory phase and the order of the HGN and PHN discharges in the inspiratory phase persisted (white regions of integrated waveforms in Fig. 8B-[2]), the TGN discharge was generated in the expiratory phase ( $r = 0.87$ ; orange-shaded regions of integrated waveforms and circular plots in Fig. 8B-[2]). The same result was

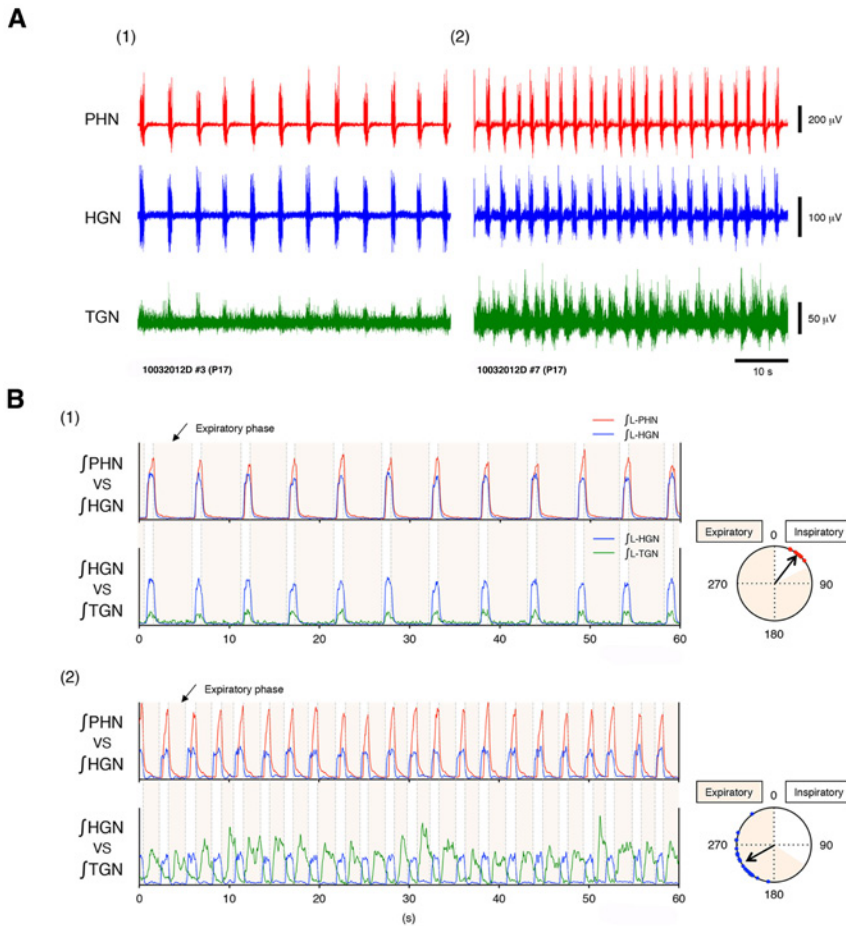


**Figure 8.** A. (1) shows typical examples of the PHN (red), HGN (blue) and TGN (green) discharges in response to a flow rate of 8x TBV/min. (2) shows discharges from all three nerves resulting from continuous administrations of 10 μM NaCN at the same flow rate, to continuously increase both the peripheral and central chemoreceptor discharges. B. (1) and (2) show the integrated waveforms of discharges from all three nerves, which correspond to A-(1) and A-(2), respectively. All data were obtained from the same preparation at postnatal 17.

obtained in five preparations. These results indicate that the shift from inspiratory phase to expiratory phase, in the opening movement in the mandible was generated by increasing peripheral and central chemoreceptor discharges.

### 8. Discharge episodes generated in both the brainstem and the spinal cord

Although the TGN discharge was generated in both the inspiratory and expiratory phases during TGN discharge episodes at the higher flow rates ( $\geq 9 \times$  TBV/min) (Figs. 6A-[2], 7A-[1] and 7B-[1]), we did not know why the TGN discharge occurred in the expiratory phase. Despite the

preparation being exposed to a hyperoxic/normocapnic state with the increasing flow rate, the amplitude of TGN discharge increased and that of HGN discharge showed an increasing trend with increasing flow rate (Fig. 6B). Strangely, these results were contradictory to the result of St. John and Bledsoe [20]. Moreover, fictive locomotion was generated in the upper limbs and the entrainments of respiratory and locomotor rhythms occurred during discharge episodes produced at  $\geq 10 \times$  TBV/min (Fig. 4). Based on these results, we tested the hypothesis that the TGN discharge, occurring in the expiratory phase, was generated by the activated cervical cord producing a left/right alternating discharge.

To examine whether the activated cervical cord production of a left/right alternating activity is generated via ascending pathways discharge episodes that were periodically seen in the PHN, MCN, HGN, and TGN discharges at  $\geq 10 \times$  TBV/min (Figs. 2A-[2], 3, 4, 5A-[2], 6A-[2], 7A-[1] and 7B-[1]), the neuronal discharges were recorded from the L-HGN and L-TGN with the same spinomedullary transected preparation as used in Fig. 5.

Figure 9-(1) shows typical examples of instances of the L-HGN and L-TGN discharges, in response to the same flow rate as used in Fig. 6B (10x TBV/min). Simultaneously, systemic pressure was monitored (data not shown). Figure 9-(2) shows the ∫L-HGN and ∫L-TGN discharges, which correspond to the neuronal discharges shown in Figure 9-(1). Using the time series data of instances of L-HGN and L-TGN discharge during discharge episodes, circular plot analysis was used to determine the phase shift within the respiratory phase between the instances of L-HGN and L-TGN discharge. All data were obtained from the same preparation made at postnatal day 11. Discharge episodes were periodically generated in both the L-HGN and L-TGN. The L-TGN was generated in the inspiratory phase ( $r = 0.97$ ; circular plots in Fig. 9-[2]). The same result was obtained in the five preparations. These results indicate that discharge episodes are not only generated in the spinal cord (Fig. 5B), but also in the brainstem, and that the activated spinal cord is producing a left/right alternating discharge that generates the TGN discharge via ascending pathways in the expiratory phase.

## Discussion

The interplay of neural discharge patterns involved in "respiration", "circulation", "opening movements in the mandible", and "locomotion" was investigated using electrophysiological techniques in a decerebrate and arterially perfused *in situ* rat preparation at 26°C. Sympathetic tone increased with increases in the perfusion flow rate. Neuronal discharges from the L-PHN, L-MCN and R-MCN, the L-HGN and L-TGN became clearly organized into "discharge episodes" of increasing frequency and duration, punctuated by quiescent

periods as the perfusion flow rate increased. Although the sympathetic tone increased with increasing flow rates, the sympathetic tone resulting from a flow rate of  $10\times$  TBV/min, which is modulated by a hyperoxic/normocapnic state, could activate the FPG and spontaneously generate a left/right alternating discharge (i.e. fictive locomotion) in the L-MCN and R-MCN during discharge episodes. The PHN discharge synchronized with the MCN discharge during discharge episodes (i.e. locomotion) and the rhythm coupling of respiration and locomotion occurred at a range of frequency ratios (i.e., 1:2 and 1:3). At  $10\times$  TBV/min, small increases in systemic pressure generated by vasoconstriction of arterioles resulting from increasing sympathetic tone in the cardiovascular center synchronized to discharge episodes (i.e. locomotion). Opening movements in the mandible, which normally occurred during the inspiratory phase at all tested flow rates, were generated in both the inspiratory and expiratory phases during discharge episodes (i.e. locomotion) at  $\geq 10\times$  TBV/min. The phase shift to the expiratory from the inspiratory phase in the opening movement in the mandible, was found to be generated by increasing amounts of peripheral and central chemoreceptor discharges. Although it was not clear whether the central mechanisms of the entrainments of respiratory and locomotor rhythms were spinal feedback because the origin of discharge episodes was not only the brainstem, but also the spinal cord, the activated spinal cord production of fictive locomotion affected the trigeminal system of the brainstem and generated the TGN discharge in the expiratory phase during discharge episodes (i.e. locomotion).

These results indicate that: (i) locomotion can be generated in a hyperoxic/normocapnic state induced by specific respiratory conditions; (ii) Although the central mechanisms for the entrainment of respiratory and locomotor rhythms could not be identified, a spinal-feedback mechanism generating fictive locomotion in the upper spinal cord contributed to generation of the opening movements in the mandible in the expiratory phase during discharge episodes (i.e. locomotion). The existence of this mechanism implies that

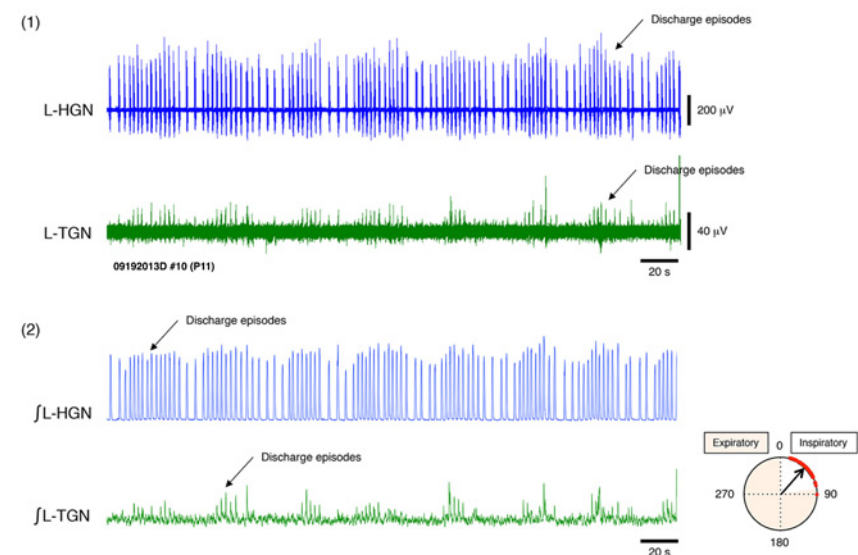


**Figure 9.** (1) Typical examples of instances of L-HGN (blue) and L-TGN (green) discharges in response to a flow rate of  $10\times$  TBV/min in the same spinomedullary transected preparation as used in Fig. 5. All data was obtained from the same preparation made at postnatal 11. (2) The J-L-HGN (blue) and J-L-TGN (green) discharges, which correspond to the neuronal discharges shown in (1). The discharge episode was periodically generated in both the L-HGN and L-TGN at the same flow rate as used in Fig. 5B ( $10\times$  TBV/min). The L-TGN (green) discharge was generated in the inspiratory phase ( $r = 0.97$ ; circular plots of [2]). Similar results were obtained in all cases ( $n = 5$ ).

there is an autonomous reciprocal functional interaction between the brainstem and the upper spinal cord, and that respiration during locomotion is performed through not only nasal breathing but also through mouth breathing, so that intake and discharge of air by the lungs is efficiently improved by shortening the airway pathways; (iii) The increase in systemic pressure generated during locomotion, implies that the elevated perfusion flow speed was produced by vasoconstriction as the perfusion flow rate was kept constant in the preparation used in this study. From the above, it is suggested that this reciprocal functional interaction plays an important role in increasing oxygenated blood flow to accommodate for the increase in metabolism generated by locomotion.

### Sympathetic/parasympathetic tone of the decerebrate and arterially perfused *in situ* preparation

In the present study, the oxygen and ion components of bodily fluid required for the survival of the preparation were supplied by the perfusate via the blood vessels, while body temperature was maintained at  $26^{\circ}\text{C}$ . When

the flow rate was high enough to produce a systemic pressure greater than 20 mmHg, the preparation showed spontaneous respiration, and when the perfusion flow rate was set at  $\geq 5\times$  TBV/min, the phrenic discharge showed an 'eupnoeic pattern' (i.e. incrementing discharge patterns) and 'regular rhythm'. The catheter was securely held in the aortic valve: the outer diameter of the tip was modified to a diameter slightly larger than that of the inner diameter of the valve. This modification ensured that the perfusate entered the ascending aorta without regurgitation into the left ventricle. The perfusate flowed from the ascending aorta to the right atrium. Thus, the blood pressure change seen in this study was generated by vasoconstriction/vasodilation. The heart did not contribute to the change in blood pressure. Also, we did not use vasoconstrictors (i.e. arginine vasopressin). When conducted in this manner, the systemic pressure of the preparation was much lower than that maintained *in situ* by other investigators. We previously reported that locomotion could be generated in a hyperoxic/normocapnic state induced by specific respiratory conditions

[12]. Fictive locomotion was generated at the sympathetic tone resulting from a flow rate of 10x but not 8x TBV/min (Figs. 4B-[1] and 4B-[2]). This difference might be attributed to the following factors: (i) the hypothermia under which the preparation was examined (i.e. at 26°C), which led sympathetic tone to be extremely low; (ii) despite increasing with increasing flow rate, the sympathetic tone seen at each high flow rate ( $\geq 10 \times$  TBV/min) was easily modulated by afferent input from the peripheral chemoreceptors, leading to a decrease in systemic blood pressure due to the hyperoxic state; and (iii) the leaking of perfusate from damaged capillaries and vessels when the preparation had been decerebrated and the skin systemically peeled. Furthermore, arginine vasopressin acts on V1 receptors to mediate vasoconstriction of peripheral blood vessels [40, 41], changing the constrictor activity of the peripheral sympathetic nervous system [42]. Therefore, the absence of arginine

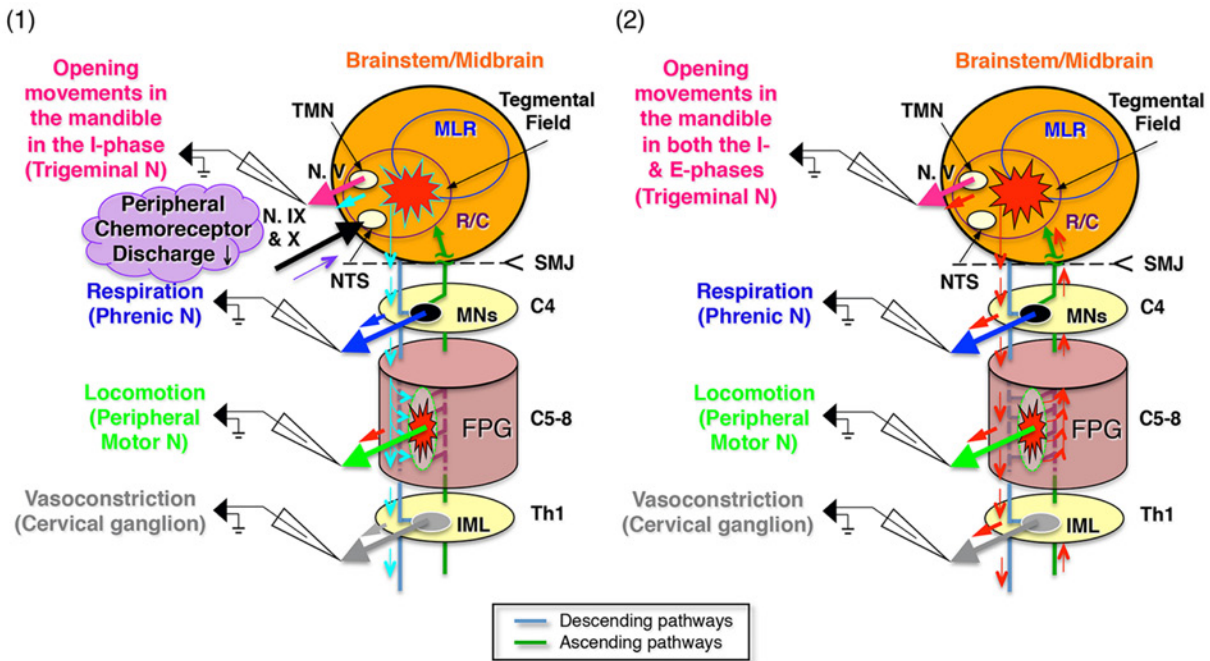
vasopressin from the perfusate could also have played a role in the lower systemic respiration of the preparation compared with that *in vivo* and in other *in situ* studies.

**Mechanism(s) of fictive locomotion induced by a hyperoxic/normocapnic state in the decerebrated and arterially perfused *in situ* preparation**

We speculate that the mechanisms for initiation of fictive locomotion seen in Figure 4B-(2) are as follows (Fig. 10-[1]): (i) the sympathetic tone resulting from a flow rate of 10x TBV/min was modulated by a hyperoxic/normocapnic state; (ii) The modulated sympathetic tone activated the FPG, located in the grey matter of the spinal cord segments C5-Th1, which produced discharge episodes consisting of a left and right synchronous discharge (Figs. 4A-[1] and 4B-[1]), and generated a left and right alternating discharge (i.e. fictive locomotion) during discharge episodes in the forelimbs.

It is known that the MLR, the respiratory/ cardiovascular networks, and the trigeminal systems are morphologically located in overlapping brainstem and midbrain areas and that locomotor-like discharges can be elicited through MLR stimulation [13–15]. However, although we do not know whether the modulated sympathetic tone is transmitted to the cervical spinal cord via the MLR or neighboring areas, sent directly to the cervical spinal cord, or sent to the cervical spinal cord via unknown pathways (Fig. 10-[1]), we believe that the descending pathway that activates the FPG is the reticulospinal pathway.

Discharge episodes consisting of a left and right synchronous discharge were alternatively generated in the L- and R-LCN of the transected preparation for a long time ( $\geq 10$  min) at  $\geq 10 \times$  TBV/min (Figs. 5B-[2] and 5B-[3]). This rhythm frequency was very slow compared with that of the intact preparation, as seen in Fig. 4B-(2). Although we tried to perfuse the hindlimb



**Abbreviations:** NTS The Nucleus of the Tractus Solitarius; R/C Respiratory/Circulatory center; TMN Trigeminal motor nuclei; MLR Mesencephalic Locomotor Region; SMJ Spino-Medullary Junction; N. IX Glossopharyngeal nerve (containing carotid sinus nerve); N. X Vagal nerve (containing Aortic nerve); N. V Trigeminal nerve; C4; The 4<sup>th</sup> Cervical spinal cord; Th 1 The 1<sup>st</sup> Thoracic spinal cord; IML; Intermediolateral nucleus; C5-8 The 5<sup>th</sup> to 8<sup>th</sup> Cervical spinal cord; FPG Forelimb Pattern Generator.

**Figure 10.** Schematic representation: (1) the modulated sympathetic tone triggers the FPG via descending pathways and generates fictive locomotion in the forelimbs, and (2) the locomotor rhythm in the cervical cord, while a left/right alternating activity occurs in the forelimbs, which entrains via ascending pathways, both the respiratory rhythm and the rhythm of the opening movements in the mandible. Simultaneously, the activated cervical cord inducing locomotion affects the cardiovascular center via ascending pathways. And then impulses in the cardiovascular center are transmitted to sympathetic chain (i.e. the cervical ganglion) via the intermediolateral cell column (IML) of the thoracic cord and the increase in systemic pressure is generated by vasoconstriction of arterioles through increased sympathetic tone.

preparation at high flow rates to activate the LPG of the lumbosacral cord of the hindlimb preparation, a left/right alternating discharge was not continuously generated in the hindlimb of the preparation. Thus, we speculate that a certain drive needs to be supplied to the upper spinal cord to trigger the FPG and continuously generate a left/right alternating activity shown in Figs. 5B-(2) and 5B-(3), and that the mechanisms for initiation of this alternating activity in our preparation are as follows: (i) The primary source of some of the drive is the sympathetic/parasympathetic tone in the brainstem; (ii) The sympathetic tone originating in the brainstem is severed by transection of the spinal cord because signals originated in the cardiovascular center are transmitted to the thoracic spinal cord through a descending pathway; (iii) The parasympathetic tone increases with increases in the flow rate, which is transmitted via the vagus nerve to the peripheral autonomic nervous system. The sympathetic tone autonomously increases with increases in the parasympathetic tone, so as to keep the balance between sympathetic and parasympathetic tone in the peripheral autonomic nervous system; (iv) The sympathetic/parasympathetic tone originating in the peripheral autonomic nervous system increases with increasing flow rates, which affects the FPG and generates a left/right alternating discharge shown in Figs. 5B-(2) and 5B-(3), although we do not know whether the sympathetic tone in the peripheral autonomic nervous system is modulated or not.

### The central mechanism(s) of reciprocal functional interactions between the brainstem and trigeminal systems during fictive locomotion

During discharge episodes resulting from a flow rate of  $10\times$  TBV/min, fictive locomotion was generated in the forelimbs (Fig. 10-[1]). Entrainments of respiratory and locomotor rhythms occurred at a range of frequency ratios (i.e. 1:2 and 1:3; Figs. 4A-[2] and 4B-[2]). If the flow rate was increased furthermore, based on the results shown in Figs. 4A-(3)

and 4B-(2), the coupling of respiratory and locomotor rhythms could be generated at about a 1:1 frequency ratio for a long time, as the extent of the modulation by the sympathetic tone increased. Small increases in systemic pressure were generated when discharge episodes resulting from a flow rate of  $\geq 10\times$  TBV/min were observed in the PHN (Figs. 2 and 3). Although this increase in systemic pressure during discharge episodes was found to be produced by vasoconstriction of arterioles resulting from increased SND, we do not know why sympathetic outflow in the cardiovascular center increased during locomotion. Opening movements in the mandible, which normally occurred during the inspiratory phase at all tested flow rates, were generated in both the inspiratory and expiratory phases during discharge episodes. This happens because fictive locomotion produced by the activated spinal cord affects the trigeminal system via ascending pathways, thus generating the opening movement in the mandible in the expiratory phase (Figs. 4A-[2], 4B-[2], 6, 7A-[1], 7B-[1], and 9). The phase shift from the inspiratory to the expiratory phase in the opening movement in the mandible, was found to be generated by increasing amounts of peripheral and central chemoreceptor discharges (Fig. 8). Moreover, despite the preparation being exposed to a hyperoxic/normocapnic state with increasing flow rate, the amplitude of TGN discharge increased (Fig. 6). This result contradicts the result published by St. John and Bledsoe [20]. We previously reported that discharge episodes were generated in the lower spinal cord and that a spinal-feedback mechanism generating a locomotor-like discharge in the lower spinal cord is the principal mechanism in the entrainment of respiratory and locomotor rhythms [12]. However, we could not identify the central mechanisms for the entrainment of respiratory and locomotor rhythms because discharge episodes originated not only in the spinal cord (Fig. 5B-[2]), but also the brainstem (Fig. 9), and the coupling of respiratory and locomotor rhythms was not generated at a 1:1 frequency ratio in this study.

Based on the results shown in Figs. 6, 7, and 9, we speculate that a spinal-feedback mechanism generating fictive locomotion in the spinal cord is the principal mechanism for the rhythm couplings of respiration, circulation, opening movement of the mandible, and locomotion, which are as follows (Fig. 10-[2]): (i) impulses in the activated cervical spinal cord inducing a left/right alternating discharge are transmitted to the respiratory center of the brainstem through ascending spinal pathways. These impulses affect not only neuron groups generating the inspiratory phase but also neuron groups generating the expiratory phase in the respiratory center. Also, they are transmitted to the trigeminal (motor) system in the brainstem. Then, opening movements in the mandible during locomotion are produced in the inspiratory and expiratory phases via the TGN; (ii) Impulses transmitted to the respiratory/circulatory center are propagated to the cardiovascular center and the sympathetic tone in the cardiovascular center increases. Consequently, blood pressure is increased during locomotion. We also speculate that a likely candidate in the brainstem pontine relay nuclei for entrainment of respiratory and locomotor rhythms is the nucleus of the tractus solitarius, which is the first relay station of the respiratory/circulatory networks for sensory information originating from various viscera [43, 44].

### Acknowledgments

Author contributions: I.Y. conceived and initiated the project. I.Y. performed experiments with rat and analyzed data. I.Y. steered the entire project, and wrote the paper. I.Y., S. S. approved the final version to be published. This work was supported by JSPS KAKENHI Grant Number 24500612. We thank Satoshi Tachikawa for technical assistance and Dr Seiji Shioda for his assistance in regard to research instruments for this research. *Conflict of interest statement:* The authors declare that the research was conducted in the absence of any commercial or financial relationships that could be construed as a potential conflict of interest.

## References

- [1] Ainsworth D.M., Smith C.A., Henderson K.S., Dempsey J.A., Breathing during exercise in dogs - passive or active?, *J. Appl. Physiol.*, 1966, 81, 586-595
- [2] Bramble D.M., Carrier D. R., Running and breathing in mammals, *Science*, 1983, 219, 251-256
- [3] Dejours P., Neurogenic factors in the control of ventilation during exercise, *Circ. Res.*, 1993, 20/21 (Suppl. 1), 1146-1153
- [4] Iscoe S., Respiratory and stepping frequencies in conscious exercising cats, *J. Appl. Physiol.*, 1981, 51, 835-839
- [5] Krogh A., Lindhard J., The regulation of respiration and circulation during the initial stages of muscular work, *J. Physiol.*, 1913, 47, 112-136
- [6] Corio M., Palisses R., Viala D., Origin of the central entrainment of respiration by locomotion facilitated by MK 801 in the decerebrate rabbit, *Exp. Brain. Res.*, 1993, 95, 84-90
- [7] Eldrige F.L., Millhorn D.E., Killey J.P., Waldrop T.G., Exercise hyperpnea and locomotion: parallel activation from the hypothalamus, *Science*, 1981, 211, 844-846
- [8] Brice A.G., Forster H.V., Pan L.G., Funahashi A., Hoffman M.D., Murphy C.L., et al., Is the hyperpnea of muscular contractions critically dependent on spinal afferents?, *J. Appl. Physiol.*, 1988, 64, 226-233
- [9] Brown D.R., Forster H.V., Pan L.G., Brice A.G., Murphy C.L., Lowry T.F., et al., Ventilatory response of spinal cord lesioned subjects to electrically induced exercise, *J. Appl. Physiol.*, 1990, 68, 2312-2321
- [10] Giraudin A., Le Bon-Jego M., Cabirol M.J., Simmers J., Morin D., Spinal and pontine relay pathways mediating respiratory rhythm entrainment by limb proprioceptive inputs in the neonatal rat, *J. Neurosci.*, 2012, 32, 11841-11853
- [11] Potts J.T., Rybak I.A., Paton J.F., Respiratory rhythm entrainment by somatic afferent stimulation, *J. Neurosci.*, 2005, 25, 1965-1978
- [12] Yazawa I., Reciprocal functional interactions between the brainstem and the lower spinal cord, *Front. Neurosci.*, 2014, 8, 124
- [13] Iwamoto G.A., Wappel S.M., Fox G.M., Buetow K.A., Waldrop T.G., Identification of diencephalic and brainstem cardiorespiratory areas activated during exercise, *Brain Res.*, 1996, 726, 109-122
- [14] Rye D.B., Lee H.J., Saper C.B., Wainer B.H., Medullary and spinal efferents of the pedunclopontine tegmental nucleus and adjacent mesopontine tegmentum in the rat, *J. Comp. Neurol.*, 1988, 269, 315-341
- [15] Skinner R.D., Garcia-Rill E., The mesencephalic locomotor region (MLR) in the rat, *Brain Res.*, 1984, 323, 385-389
- [16] Holstege J.C., Kuypers H.G., Brainstem projections to spinal motoneurons: an update, *Neuroscience*, 1987, 23, 809-821
- [17] Grillner S., Control of locomotion in bipeds, tetrapods, and fish, In: *Handbook of physiology, Section 1: The nervous system, Vol. 2*, Brookhart J.M., Mountcastle V.B. (Eds.), American Physiological Society, Bethesda, MD, USA, 1981, 1179-1236
- [18] Feldman J.L., Neurophysiology of breathing in mammals, In: *Handbook of physiology, Intrinsic regulatory systems, Vol. 4*, Bloom F.E. (Ed.), American Physiological Society, Bethesda, MD, USA, 1986, 463-524
- [19] Nakamura Y., Takatori M., Kubo Y., Nozaki S., Enomoto S., Masticatory rhythm formation - facts and a hypothesis, In: *Integrative control functions of the brain, Vol. 2*, Tsukahara K., Kubo S., Yagi K. (Eds.), Kodansha Scientific, Tokyo, Japan, 1979, 321-331, 1979
- [20] St. John W.M., Bledsoe T.A., Comparison of respiratory-related trigeminal, hypoglossal and phrenic activities, *Respir. Physiol.*, 1985, 62, 61-78
- [21] Pickering A.E., Paton J.F., A decerebrate, artificially-perfused in situ preparation of rat: utility for the study of autonomic and nociceptive processing, *J. Neurosci. Methods*, 2006, 155, 260-271
- [22] Fox L.S., Blackstone E.H., Kirklin J.W., Stewart R.W., Samuelson P.N., Relationship of whole body oxygen consumption to perfusion flow rate during hypothermic cardiopulmonary bypass, *J. Thorac. Cardiovasc. Surg.*, 1982, 83, 239-248
- [23] Kirklin J.W., Barratt-Boyes B.G., Hypothermia, circulatory arrest, and cardiopulmonary bypass, In: *Cardiac surgery*, Kirklin J.W., Barratt-Boyes B.G. (Eds.), Churchill Livingstone, New York, NY, USA, 1993, 61-127
- [24] Harkness J.E., Wagner J.E., Biology and husbandry, In: *The biology and medicine of rabbits and rodents*, Harkness, J.E., Wagner J.E. (Eds.), Lea & Febiger, Philadelphia, PA, USA, 1989
- [25] Mitruka B.M., Rawnsley H.M., Clinical biochemical and hematological reference values in normal experimental animals and normal humans, Masson, New York, NY, USA, 1981
- [26] Barman S.M., Gebber G.L., Basis for synchronization of sympathetic and phrenic nerve discharges, *Am. J. Physiol.*, 1976, 231, 1601-1607
- [27] Coleridge H.M., Coleridge J.C., Cardiovascular afferents involved in regulation of peripheral vessels, *Annu. Rev. Physiol.*, 1980, 42, 413-427
- [28] Julius S., Nesbitt S., Sympathetic overactivity in hypertension. A moving target, *Am. J. Hypertens.*, 1996, 9, 1135-1205
- [29] Ballion B., Morin D., Viala D., Forelimb locomotor generators and quadrupedal locomotion in the neonatal rat, *Eur. J. Neurosci.* 2001, 14, 1727-1738
- [30] Katakura N., Jia L., Nakamura Y., NMDA-induced rhythmical activity in XII nerve of isolated CNS from newborn rats, *Neuroreport*, 1995, 6, 601-604
- [31] Naganuma K., Inoue M., Yamamura K., Hanada K., Yamada Y., Tongue and jaw muscle activities during chewing and swallowing in freely behaving rabbits, *Brain Res.*, 2001, 915, 185-194
- [32] Nakamura Y., Katakura N., Generation of masticatory rhythm in the brainstem, *Neurosci. Res.*, 1995, 23, 1-9
- [33] Batschelet E., Circular statistics in biology, In: *Mathematics in biology*, Sibson R., Cohen J.E. (Eds.), Academic Press, London, UK, 1981
- [34] Ballantyne D., Scheid P., Central chemosensitivity of respiration: a brief overview, *Respir. Physiol.*, 2001, 129, 5-12
- [35] Loeschcke H.H., Central chemosensitivity and the reaction theory, *J. Physiol.*, 1982, 332, 1-24

- [36] Nattie E.E., Central chemoreceptors, pH, and respiratory control, In: pH and brain function, Kaila K., Ransom B.R. (Eds.), Wiley-Liss Inc., New York, NY, USA, 1982, 535-560
- [37] O'Regan R.G., Majcherczyk S., Role of peripheral chemoreceptors and central chemosensitivity in the regulation of respiration and circulation, *J. Exp. Biol.*, 1982, 100, 23-40
- [38] Tenney S.M., Ou L.C., Ventilatory response of decorticate and decerebrate cats to hypoxia and CO<sub>2</sub>, *Respir. Physiol.*, 1977, 29, 81-92
- [39] Macey P.M., Richard C.A., Rector D.M., Harper R.K., Harper R.M., State influences on ventral medullary surface and physiological responses to sodium cyanide challenges, *J. Appl. Physiol.*, 2000, 89, 1919-1927
- [40] Martin de Aguiler E., Vila J.M., Irurzun A., Martinez M.C., Martinez Cuesta M.A., Lluch S., Endothelium-independent contractions of human cerebral arteries in response to vasopressin, *Stroke*, 1990, 21, 1689-1693
- [41] Medina P., Acuna A., Martinez-Leon J.B., Otero E., Vila J.M., Aldasoro M., et al., Arginine vasopressin enhances sympathetic constriction through the V1 vasopressin receptor in human saphenous vein, *Circulation*, 1998, 97, 865-870
- [42] Bartelstone H.J., Nasmyth P.A., Vasopressin potentiation of catecholamine actions in dog, rat, cat and rat aortic strip, *Am. J. Physiol.*, 1965, 208, 754-762
- [43] Kalia M., Sullivan J.M., Brainstem projections of sensory and motor components of the vagus nerve in the rat, *J. Comp. Neurol.*, 1982, 211, 248-265
- [44] Yazawa I., Intrinsic optical imaging of neural activity induced by vagal stimuli in the in vivo rat brainstem: the possibility of a distributed organization of the NTS, *FASEB J.*, 2005, 19, A597